Introduction

Nanophthalmos is a rare congenital ocular disorder, included in the spectrum of developmental eye diseases, characterized by a small eye, due to a compromised eye growth after the closure of the embryonic fissure[1]. Nanophthalmos is derived from the Greek word *nano*, meaning dwarf, and nanophthalmic eyes typically exhibit very high to extreme axial hyperopia and lack overt structural defects[2,3].

Several modes of inheritance have been described in the literature, namely autosomal dominant and recessive[3,4,5]. Data derived from linkage studies and the identification of genetic mutations, as the cause of non-syndromic and syndromic nanophthalmos, have been of great value towards the clarification of the pathophysiology behind these conditions[6].

Two loci for autosomal dominant nanophthalmos (NNO1 and NNO3) have been identified[4,6]. The NNO1 locus maps to chromosome 11p while the NNO3 locus (OMIM #611897) maps to chromosome 2q11-q14. Autosomal recessive nanophthalmos (NNO2) (OMIM #609549) can be caused by mutations in the *MFRP* gene (OMIM #606227) on chromosome 11q23[5].

Sundin et al. (2005) performed linkage analysis using DNA samples from 16 members of the Amish-Mennonite kindred originally reported by Cross and Yoder (1976), including 5 individuals with nanophthalmos[3,5]. Mutations in the membrane-type frizzled related protein (MFRP) gene were identified as the cause of classic non-syndromic Mendelian recessive nanophthalmos[5].

MFRP has 13 exons, which translate into 579 aminoacids. The resulting protein consists of three domains: a transmembrane domain with homology to the frizzled

family of proteins, containing two cubilin domains; a low density lipoprotein receptor a; and a cysteine-rich domain, that can bind with wingless type proteins (WNTs), which might be involved in eye development, through mediating cell growth[7].

The MFRP protein is selectively expressed in the retinal pigment epithelium (RPE) and the ciliary body, with low expression in the brain. It is also known that MFRP is concentrated towards the apical side of the RPE, with virtually none in Bruch's membrane. Patients completely lacking MFRP protein have no pathology outside of the eye[1]. In the fetal eye, at 7 weeks gestation, no MFRP signal is detected in the RPE. A distinct signal is observed in the RPE at 20 weeks gestation which indicates that MFRP expression begins relatively late during formation of the eye[1].

Regarding the function of MFRP, it seems to be essential for the eye to reach its full size at birth, and also for a correct emmetropization, since it is associated with regulation of ocular axial growth[1]. On the other hand, there is some controversy regarding its value in retinal function. While Sundin et al. (2008) stated that the MFRP protein is not essential for retinal function, Ayala-Ramirez et al. (2006) showed that it is necessary for photoreceptor maintenance, due to the severe rod-cone dystrophy observed in their patients[1,8].

Usually bilateral and symmetrical, nanophthalmos is characterized by a small eye, associated with: shortened axial length (21mm or less), high corneal curvature, narrow iridocorneal angle, high hyperopia (ranging from +8.00 to +25.00) and excessive thickening of both choroidal and scleral layers[1]. Patients with nanophthalmos usually feature a small eye, deeply-set in the orbit (enophthalmos) and covered by narrow palpebral fissures; bilateral mild ptosis may also be present[2,3].

Refractive analysis displays high to extreme hypermetropia[2,3]. In children, both eyes usually exhibit extreme axial hyperopia but are highly functional; correction with glasses that resemble aphakic spectacles usually results in moderate to good visual acuities. Evaluation of the total axial length demonstrates reduced values (usually ranging from 14 to 20.5 mm), smaller equatorial and transverse diameters resulting in a reduced total ocular volume[9,10].

Slit-lamp examination reveals a transparent cornea with diameters ranging from 9 to 11.5 mm, spanning from the microcornea range to normal values. Keratometric evaluation reveals higher, regular, corneal curvatures with or without astigmatism. A shallow anterior chamber and narrow iridocorneal angle result from a normal sized transparent lens that occupies a disproportionately large percentage of intraocular volume. As a consequence, the presence of a prominent iris convexity and impending angle closure with peripheral anterior synechiae (that may eventually form) may be observed beyond the fourth decade[10,11].

Fundus examination may reveal a normal posterior segment. The discs may be normal or appear crowded, or display the infrequent finding of disc drusen[5]. A variety of macular and peripheral retinal findings have been described; these include varying degrees of macular hypoplasia, rudimentary foveal avascular zone[12], foveal cysts, foveal schisis-like changes[13], and small yellowish deposits in the mid-periphery[5]. Additional reported retinal manifestations include a retinitis pigmentosa-like phenotype, a pigmentary retinal dystrophy[14]. Since the choroid and sclera are usually thickened, the nanophthalmic eye is predisposed to the development of choroidal effusions and nonrhegmatogenous retinal detachments[14].

Structural analysis using optical coherence tomography (OCT) may reveal diffuse macular thickening, schisis of the outer retinal layers with discrete bridging elements at the fovea, absence of foveal pit, or evidence of macular cysts or cystic-like changes. Functional retinal testing including electroretinography (ERG) varies from normal responses to variable degree of photopic and scotopic dysfunction[5].

Additional findings may include nystagmus and strabismus, usually nonaccommodative esotropia[15]. A common finding is the observation of either monocular or binocular amblyopia.

Heterozygote patients without nanophthalmos studied by Sundin et al. (2005) showed no hyperopia; however, some features like corneal curvature and anterior chamber depth revealed semidominance by being significantly altered comparing to the general population. Despite these abnormalities, the eye has no overt structural defects and the retina has normal function, appearing superficially normal at birth. The visual acuity defects presented by some patients are usually the result of additional complications, such as angle closure glaucoma (normal sized lens blocks the outflow of aqueous humor), cystic edema, retinal folds and/or detachment (thickened sclera blocks the outflow vessels from the choroid layer, leading to transudation between the RPE and the neural retina), and retinitis pigmentosa[5]. Thus, nanophthalmos can be an isolated disorder, or be part of a syndrome, such as the "nanophthalmos, retinitis pigmentosa, foveoschisis and optic drusen syndrome"[8], the "oculo-dento-digital syndrome"[16], "autosomal dominant vitreoretinochoroidopathy with nanophthalmos"[17] and the "Kenny-Caffey syndrome"[18].

Objectives

We propose to characterize from a phenotypical standpoint twelve individuals from eleven unrelated families (five males, seven females, ages between 5 and 78 years) with nanophthalmos, determine if they carry MFRP mutations, and establish potential genotype-phenotype correlations, both with respect to corneal and retinal structural and changes, using corneal topography (Orbscan) and spectral-domain OCT.

Materials and Methods

Patient and control population

Twelve individuals from eleven unrelated families (five males, seven females, ages between 5 and 78 years) were included in this study. All affected individuals are followed at the Centre for Hereditary Eye Diseases of the Department of Ophthalmology, University Hospital of Coimbra. Probands and affected family members presented at our clinic mostly due to visual impairment (loss of central vision), extreme or very high hyperopia and/or funduscopic changes that fit the clinical diagnosis of nanophthalmos.

All individuals included in the study were informed about its objectives and volunteered to participate. Informed consent was obtained from all subjects according to the tenets of the declaration of Helsinki. The study was approved by the Ethics Committee of the University Hospital of Coimbra.

Clinical Examination

Ophthalmic examination included assessment of best corrected visual acuity (BCVA) after manifest or cycloplegic refraction, slit-lamp examination, fundus

examination using a non-contact 78-diopter lens. Fundus photography was performed with a TOPCON TRC 50X (Topcon Optical, Tokyo, Japan).

Optical Coherence Tomography (OCT)

We used an OCT device (Stratus OCT; Carl Zeiss Meditec, Dublin, CA; Spectralis OCT, Heidelberg, Germany) to obtain cross-sectional images centered in the macula,26 with axial resolution of 10 _m or less, transversal resolution of 20 _m, and longitudinal scan range of 2 mm. With this OCT device (Stratus OCT; Carl Zeiss Meditec), six radial line scans 6 mm in length and 128 A-scans 30° apart were scanned in 1.92 seconds, and a nine-region retinal thickness map was obtained by segmenting the retina from other layers with an algorithm detecting the edge of the RPE and the photoreceptor layer.

Macular retinal thickness was calculated by computing the distance between the signal from the vitreoretinal interface and the signal from the anterior boundary of the RPE. Retinal thickness was presented as a nine-region thickness map showing the interpolated thickness for each area, with a central circle of 500 _m radius (ring 0) and two outer circles with radii of 1500 _m (ring 1) and 3000 _m (ring 2). The interpolated thickness was displayed using a false color scale, in which bright colors (red and white) corresponded to thickened areas and darker colors (blue and black) were assigned to thinner areas.

ORBScan

Computerized videokeratography (Orbscan® IIz; Bausch and Lomb Inc., Rochester, NY, USA) was obtained, and the following topographic parameters were noted: simulated keratometry (Sim K) astigmatism; irregularities and mean refractive powers in the central and 3 mm zones; and steep astigmatic axes.

The examination process begins with entering basic information, proper positioning of patient head, forehead, and chin, and adjusting the instrument. During data acquisition, 20 slits are projected onto the cornea from each side for a total of 40 slits. This is done in a scanning fashion at an angle of 45 degrees, and the backscattered light is captured by a digital video camera. Data from 240 points are extracted from each slit, and processed by the software to calculate different variables. The most common display is the "quadmap" that includes 2-dimmensional color-coded maps of the anterior and posterior corneal surface elevation, the corneal thickness or pachymetry map, and the corneal curvature or power map.

Molecular genetic analysis

Genomic DNA was extracted using an automated DNA extractor (BioRobot EZ1, Qiagen, Hilden, Germany). The 13 exons of gene *MFRP* were PCR-amplified using previously described primers and conditions (Sundin *et al*., 2000). Amplification products were purified with QIA-quick Gel Extraction Kit (Qiagen). Sequencing reactions were performed using the 4-dye terminator cycle sequencing ready reaction kit (BigDye DNA Sequencing Kit, Applied Biosystems, Foster City, CA). Sequence products were purified through fine columns (Sephadex G-501, Princetown Separations, Adelphia, NJ) and resolved in an ABI Prism 3130 (Applied Biosystems).

Results

***Clinical phenotype**:*

The clinical data of the twelve patients are detailed in Table I. The age of the patients studied ranged between 5 and 78 years, with an average age of 34,6 years, and there were seven females and five males.

Best-corrected visual acuity of the better eye was less than or equal to 5/10 in eleven patients; only one patient had visual acuity better than 5/10 (NAN 11). One patient (NAN 6) has less than 1/10, due to closed-angle glaucoma.

All twelve patients were highly hypermetropic, with ***spherical equivalents*** ranging between +8.50 diopters (D) and +24.00 D, with an average of 14,375 D. By questionnaire, all patients denied the presence of significant refractive error, in the hyperopic range, in their parents.

Regarding the ***corneal measurements***, four patients had a normal (11mm) corneal diameter (NAN 3, 4, 5 and 7) and five patients (NAN 1, 2, 6, 8, 9 and 11) had a sub-normal diameter, ranging from 9,5 to 10,5mm. We couldn't perform the examination on the two remaining patients (NAN 10).

Retinal examination revealed preservation of central macular reflex in almost all patients (except NAN 2, 7 and 9). Seven patients (NAN 1, 2, 3, 4, 5, 7 and 8) presented crowded discs (Figure 1). One patient (NAN 9) developed a retinal detachment involving the macular area. Yellowish deep retinal deposits (flecks) were presented in three (NAN 4 and 10) of the twelve patients (Figure 2). Two patients presented with macular cysts (NAN 2 and 7). One of the patients presented with pseudopapiledema

(NAN 5) and one other with a macular fold in the right eye (NAN 7). Only one patient presented with normal posterior eye segment.

Table I – Clinical Features

Family	Age	Gender	RE (spherical equivalent)	Corneal diameter (mm)		BCVA		Posterior segment findings	Additional information
				OD	OS	OD	OS		
NAN 1	7	Female	9	10,5	10,5	2/10	2/10	crowded discs	
NAN 2	16	Male	13	10,5	10,5	5/10	5/10	Macular cysts; crowded discs	
NAN 3	15	Male	13	11	11	4/10	3/10	crowded discs	
NAN 4	47	Male	8,5	11	11	5/10	5/10	Yellow flecks; crowded discs	
NAN 5	5	Male	13	11	11	5/10	5/10	Pseudopapiledema; crowded discs	
NAN 6	53	Female	15	9,5	9,5	< 1/10	<1/10	N/A	Glaucoma + vitrectomy + trabeculectomy
NAN 7	58	Male	16	11	11	2/10	1/10	Macular cyst, crowded disc; macular fold OD	
NAN 8	78	Female	13	10	10	5/10	5/10	crowded disc; RPE atrophy	
NAN 9	60	Female	15	9,5	9,5	2/10	3/10	Exudative RD involving the macular area	
NAN 10	31	Female	24	N/A	N/A	2/10	2/10	Yellow flecks	
	34	Female	22	N/A	N/A	3/10	3/10	Yellow flecks	
NAN 11	19	Female	11	10	10	6/10	8/10	Normal	Esotropia (surgery)

RE – Refractive error ; OD – Right eye; OS – Left eye; BCVA – Best corrected visual acuity;
RPE – Retinal pigment epithelium; RD – Retinal detachment

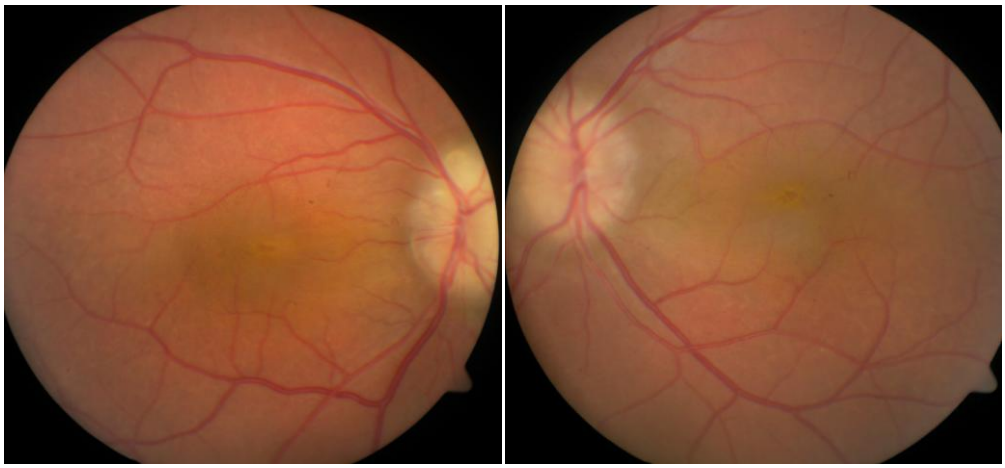

Fig.1 – Crowded discs (patient from family NAN 2)

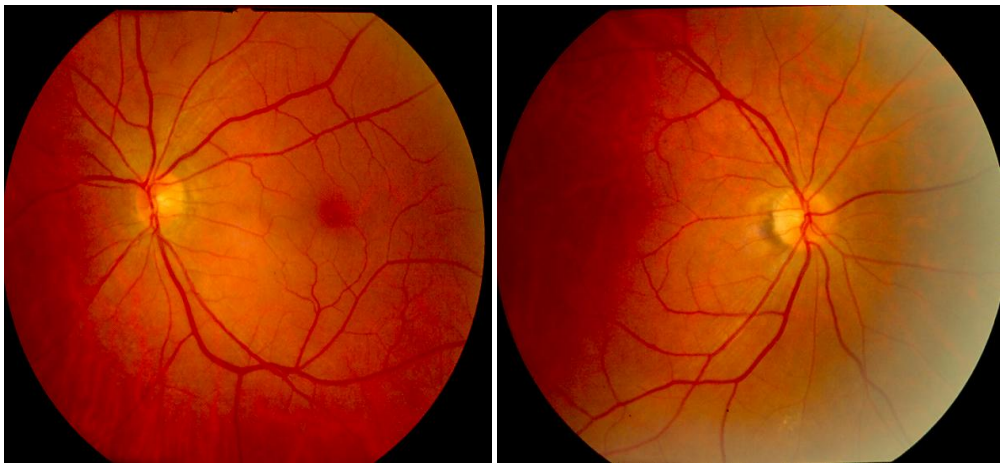

Fig.2 – Yellowish deep retinal deposits (patient from family NAN 10)

OCT examination (Table II) was performed in 14 eyes of seven patients (NAN 2, 3, 5, 7, 8, 9, 11) and revealed cystic spaces at the fovea (Figure 3), with relative preservation of the photoreceptor-retinal pigment epithelium complex in three of those patients (NAN 2, 7 and 9), as well as loss of foveal depression with no cystic areas (Figure 4) in three of the studied patients (NAN 3, 5 and 8). One (NAN 11) of the patients presented a normal retina, with no cysts and normal foveal depression.

The foveal thickness varied from 336 µm to 537 µm and the thickness at 3mm from the fovea ranged from 324,75 µm to 451 µm. In one case (NAN 5) we could only obtain the descriptive result from the retina, but not the analytical result of the retinal thickness.

Table II – OCT results

Family	OD			OS		
	Image Description	**Central (µm)**	**x 3mm (µm)**	**Image Description**	**Central (µm)**	**x 3mm (µm)**
NAN 1	N/A	N/A	N/A	N/A	N/A	N/A
NAN 2	Cysts	535	403	Cysts	537	413
NAN 3	Loss of foveal depression, no cysts	478	448	Loss of foveal depression, no cysts	490	442
NAN 4	N/A	N/A	N/A	N/A	N/A	N/A
NAN 5	Loss of foveal depression, no cysts	N/A	N/A	Loss of foveal depression, no cysts	N/A	N/A
NAN 6	N/A	N/A	N/A	N/A	N/A	N/A
NAN 7	Cysts	425	325	Cysts	495	N/A
NAN 8	Loss of foveal depression, no cysts	346	334,5	Loss of foveal depression, no cysts	357	324,75
NAN 9	Cysts	446	369,25	Cysts	520	451
NAN 10	N/A	N/A	N/A	N/A	N/A	N/A
NAN 11	No cysts and normal foveal depression	343	355,5	No cysts and normal foveal depression	336	349,5

OD – Right eye; OS – Left eye; N/A – not available

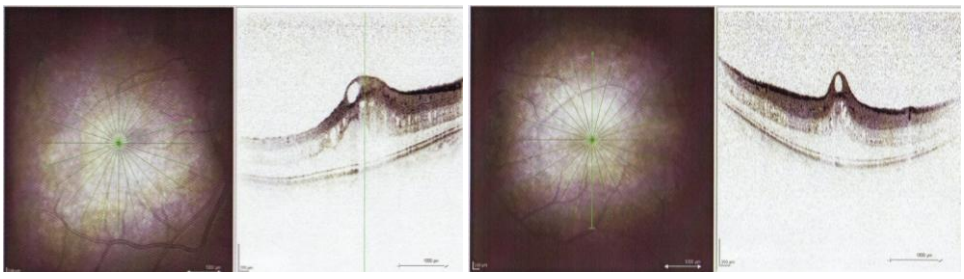

Fig.3 – Foveal cysts (NAN 2)

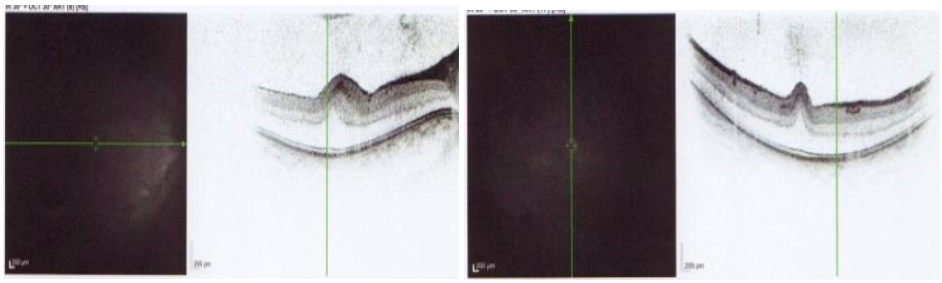

Fig.4 – Loss of foveal depression with no cystic areas (NAN 5)

ORBScan (table III; Figure 5): We performed this test in 12 eyes (NAN 2, 3, 5, 8, 9 and 11) of six patients. Regarding central corneal thickness, the results varied from 529 to 614 μm, with an average result of 538,9 μm. The maximum diopter values ranged from 48,9 to 51,6 D, with an average of 49,7 D; and the minimum values ranged from 48 to 50,1 D, with an average of 48,7 D. The results from the left eye of the subject from family NAN 8 were not used, due to lack of cooperation and consequently faulty results.

Table III– ORBScan results

Family	OD					OE				
	Central	**Max**	**Min**	**Max (D)**	**Min (D)**	**Central**	**Max**	**Min**	**Max (D)**	**Min (D)**
NAN 1	N/A	N/A	N/A	N/A	N/A	N/A	N/A	N/A	N/A	N/A
NAN 2	614	722	614	49,8	48,2	610	696	610	49,2	48
NAN 3	603	719	603	49,2	48,8	607	752	607	49,7	48,9
NAN 4	N/A	N/A	N/A	N/A	N/A	N/A	N/A	N/A	N/A	N/A
NAN 5	609	679	609	49,2	48,2	605	688	566	49,1	48,5
NAN 6	N/A	N/A	N/A	N/A	N/A	N/A	N/A	N/A	N/A	N/A
NAN 7	N/A	N/A	N/A	N/A	N/A	N/A	N/A	N/A	N/A	N/A
NAN 8	562	591	486	X	X	529	599	524	51,6	49,8
NAN 9	587	668	587	51,1	50,1	565	686	565	49,4	48,6
NAN 10	N/A	N/A	N/A	N/A	N/A	N/A	N/A	N/A	N/A	N/A
	N/A	N/A	N/A	N/A	N/A	N/A	N/A	N/A	N/A	N/A
NAN 11	561	645	561	48,9	48,2	555	684	555	49,1	48,7

OD – Right eye; OS – Left eye; D – diopter; N/A – not available; X – data excluded

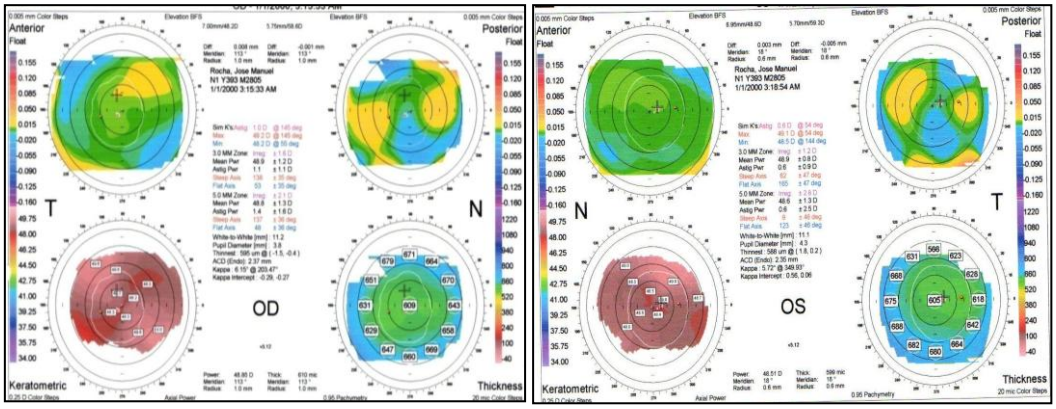

Fig.5 – ORBScan (NAN 5)

Molecular genetics (table IV)*:* Pedigrees of each of the families are illustrated in Figure 6. Direct sequencing of the *MFRP* amplicons in affected members of the remaining families revealed several mutations, three of which were novel (IVS6-1G>C, IVS8-1G>A and c.661insC).

The proband of family NAN 8 was a compound heterozygous for one known (c.1143ins C) [Sundin et al. (2005)] and one novel mutation (IVS8-1G>A) in intron 8. The patients in families NAN 7 and 11 were heterozygous for two novel mutations (IVS6-1G>C and c.661insC, in intron and exon 6, respectively). The remaining patients have previously described mutations [Sundin *et al.* (2005)]. The 15 year old boy from family NAN 2 was homozygous for c.523C>T, a mutation in exon 5, whereas each parent was heterozygous for the same mutation [Sundin et al. (2005)]. Affected individuals in family NAN 10 were compound heterozygous for 1-base pair deletion, c.492delC, and an aminoacid substitution, ile182thr, both in exon 5. Their father was heterozygous for the ile182thr mutation, whereas the mother was heterozygous for the c.492delC mutation [Sundin *et al.* (2005)]. No mutations were found in the affected member of family NAN 1, and the results from families NAN 4 and 6 are still pending.

Table IV– Molecular analysis

Família	Age	Gender	Mutations	Status	Exon	Protein	Consanguinity	Reference
NAN 1	7	Female	NIM					
NAN 2	16	Male	c.523C>T	Homozygous	5	p.gln175ter	No	Sundin et al. (2005)
NAN 3	15	Male	c.1143ins C	Homozygous	10	p.His384Pro fs8X	No	Sundin et al. (2005)
NAN 4	47	Male	Pending			Yes		
NAN 5	5	Male	c.492del C + c.1143ins C	Compound heterozygous	5+10	p.Asn167Thr fs 25X+ p.His384Pro fs8X	No	Sundin et al. (2005)
NAN 6	53	Female	Pending					
NAN 7	58	Male	IVS6-1G>C	Heterozygous	Intron 6		No	Novel
NAN 8	78	Female	IVS8-1G>A + c.1143ins C	Compound heterozygous	Intron 8+ 10	p.His384Pro fs8X	No	Novel+ Sundin et al. (2005)
NAN 9	60	Female	c.492del C	Heterozygous	5	p.Asn167Thr fs25X	Yes	Sundin et al. (2005)
NAN 10	31	Female	c.492delC + ile182-to-thr	Compound heterozygous	5+5	p.Asn167Thr fs25X+ p.ile182thr	No	Sundin et al. (2005)
	34	Female	c.492delC + ile182-to-thr	Compound heterozygous	5+5	p.Asn167Thr fs25X+ p.ile182thr	No	Sundin et al. (2005)
NAN 11	19	Female	c.661insC	Heterozygous	6		No	Novel

NIM - no identifiable mutation

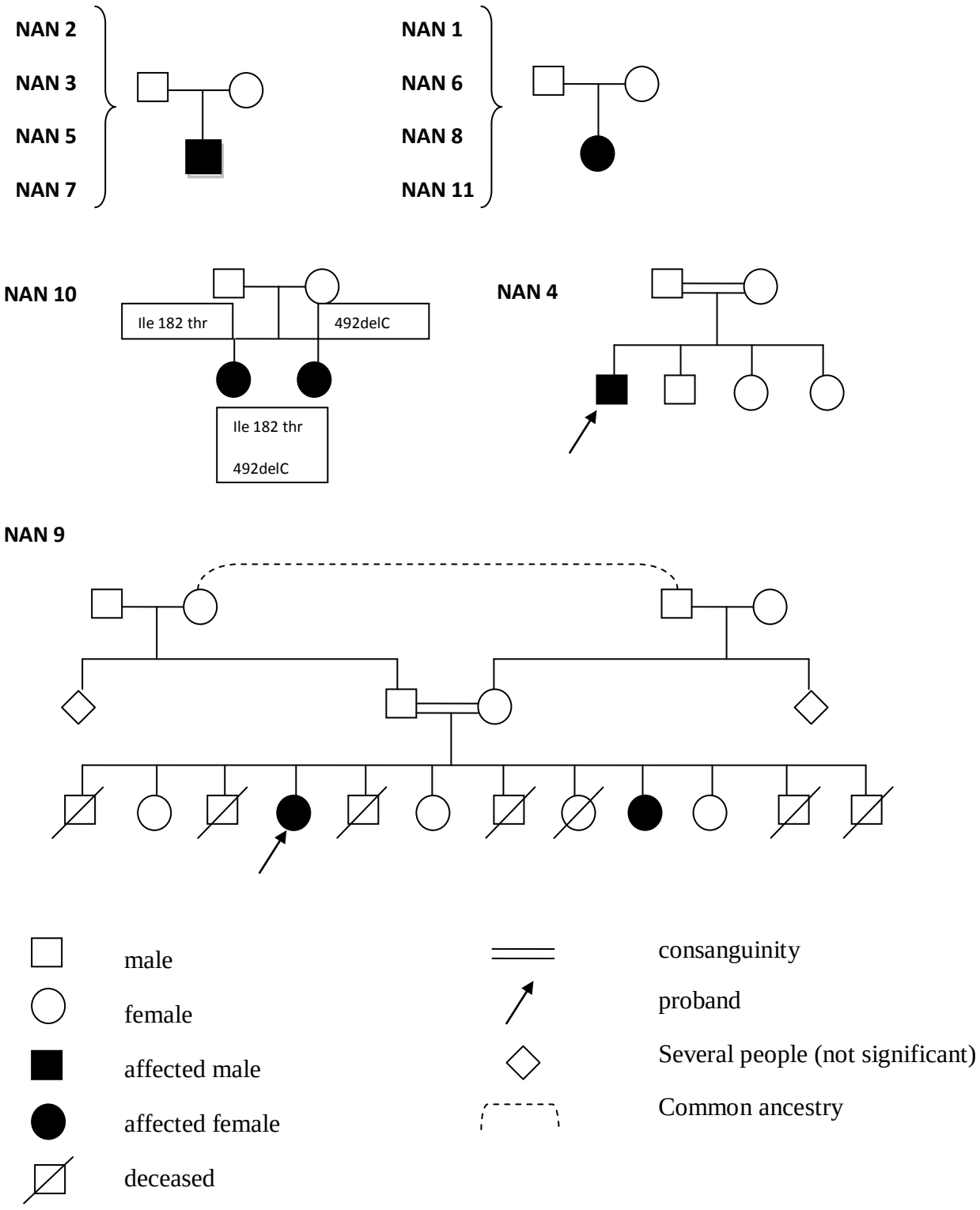

Figure 6 – Pedigree of families NAN 1-11 (with the mutations in case of NAN 10, since the parents were studied)

Discussion

After screening all 13 exons of the *MFRP* gene, the probands can be divided into four different categories: missense (carrying a missense mutation), where probands from families NAN 2 and 7 are included; frameshift (carrying a frameshift mutation), which contains the affected individuals from families NAN 3, 9 and 11; compound (those who carry a double heterozygous compound mutation), including probands from families NAN 5, 8 and 10;. The last category (NIM – no identifiable mutation) includes only NAN 1 whose proband carried no mutations in the coding region of *MFRP*.

We identified the same mutation in subjects from three independent families. Thus, the frameshift insertion, c.1143ins C, first described by Sundin *et al.* (2005), was identified in the probands from families NAN 3, 5 and 8; likewise the c.492delC mutation, first described by Sundin et al. (2005), was present in the patients from families NAN 5, 9 and 10. These results reinforce those shown by Sundin *et al.*, who proposed exons 5 and 10 as mutational hotspots.

The c.1143ins C mutation allele codes for a truncated the protein at glycine 383 and adds seven frameshift codons; this change is not found in 750 normal controls (Sundin *et al.*, 2005). All patients who carry this mutation either are homozygous (NAN 3) or coumpound heterozygous (NAN 5 and 8), which is different from what was described by Sundin et al., whose study showed a heterozygous patient, with no other mutation in *MFRP*.

The frameshift deletion 492delC truncated MFRP in one of the cubilin domains and removed the cysteine-rich domain (CRD), and it was not found in 118 normal Caucasians. The individuals we studied are either heterozygous (NAN 9) or compound

heterozygous (patient from NAN 5 also presents with the mutation c.1143ins C; both patients from family NAN 10 carried the ile182-to-thr missense mutation.

The probands from families NAN 9 and NAN11 are heterozygous for a frameshift mutation. The simplest explanation is the presence of a second MFRP mutant allele in an intronic regulatory unit or in the promoter region, disabling the normal transcription process, or a second mutant allele deleted and thus not detected by sequencing. To ascertain the latter, MLPA analysis should be performed. Other possibilities include the presence of a semidominant trait with partial penetrance due to gene dosage and/or unknown genetic or environmental factors, or a rare somatic crossover or uniparental disomy of chromosome 11 in early embryonic development that might have allowed the mutations to remain homozygous in the RPE, while leaving the locus heterozygous in the buccal epithelium and blood. In the case that MFRP is not solely implicated in these phenotypes, we can allow for other possibilities to explain the heterozygosity, such as, digenic inheritance, with double heterozygosity of two interacting mutations, one in MFRP and the other one in another, yet unidentified gene.

In family NAN 9 a spherical equivalent of 15 diopters resulting in a BCVA of 2/10 OD and 3/10 OS at age 60, absence of foveal pit (retinal detachment involving the macular area) and presence of foveal cysts, suggests that the second mutant allele doesn't retain much MFRP function or was deleted/silenced (haploinsufficiency).

As for NAN 11 a spherical equivalent of 11, BCVA of 6/10 OD and 8/10 OS, with no posterior segment findings and a normal fovea with no cysts according to the OCT results, suggests that the second mutant allele retains some MFRP function.

Another case of heterozygosity is the NAN7 proband who carries an intronic mutation IVS6-1G>C.; the same is observed for the NAN8 proband who carries another intronic mutation IVS8-1G>A. Intronic mutations may have a "read-through effect",

with no alteration of the resulting protein, or they may be splice-site mutations, resulting in a different protein due to the presence of transcripted intronic material in the mRNA. This resulting protein can either be elongated or truncated. Since the NAN 7 proband has a spherical equivalent of +16,00 and a BCVA of 2/10 OD and 1/10 OS, with a macular fold and foveal cysts, we can infer that if MFRP is implicated in these changes, the intronic mutation has some effect in the resulting MFRP protein. As for the affected member of NAN 8, the spherical equivalent of +13,00 with a BCVA of 5/10 in both eyes, RPE atrophy and loss of foveal pit also suggests that the mutation is implicated in the phenotype. The different explanations for the heterozygosity are discussed above.

Regarding the NIM family, the most likely explanation involves another gene in the determination of the nanophthalmic phenotype.

In an attempt to establish a genotype-phenotype correlation for the anatomical corneal and retinal changes, Orbscan and spectral-domain OCT were used, respectively. Foveal cysts were identified in both homozygous missense mutation probands, but also in the NAN9 proband who carries the c.492delC frameshift mutation. Loss of foveal depression with no cysts is observed in NAN5 and 8, both belonging to the compound group, but also in NAN3, who carries a frameshift mutation. No specific retinal finding was found to be exclusive of one genetically defined category. Thus, nanophthalmos is characterized by a variability of posterior segment changes[27] with no genotype-phenotype correlation regarding those changes.

In accordance with Hashemi H *et al.* (2009) we defined normal central corneal thickness (CCT) as 555.6 +/- 39.9 μm, and the thinnest thickness as 550.7 +/- 40.6 μm. Our probands were divided accordingly; affected subjects from NAN 2, 3 and 5 have CCT values higher than normal, as well as the thinnest thickness higher than normal. All three subjects have ages under 20 years, which can be one of the reasons for these

higher values, but shouldn't be responsible for values outside of the normal limits. Both patients from families NAN 3 and 5 have the frameshift mutation c.1143insC (NAN 3 homozygous and NAN 5 compound heterozygous), which could be responsible for the phenotype. On the other hand, also the NAN8 proband carries the same mutation, but normal CCT values. One possible explanation is that for this last subject, the coumpound heterozigosity with the intronic mutation IVS8-1G>A could have no influence in the corneal thickness, thus making this subject heterozygous for the c.1143insC mutation, and allowing him to have a normal corneal phenotype.

The novel mutation c.661insC (NAN 11) probably does not influence corneal thickness, as the affected patient has normal CCT values. This result is in accordance with the observation made above, where we suggest that one mutated allele alone allows for some MFRP function from the other wild-type allele. However, the same does not apply to the NAN9 proband who displays normal CCT values, but the remaining phenotype suggests that the second mutant allele doesn't retain much MFRP function or is silenced. All probands with exon 5 and 10 *MFRP* mutations have abnormally high CCT values. This probably has little significance, as most mutations arise in these two mutational hotspots. No specific trend of corneal thickness was found to correlate with one of the genetically defined categories. As a final note, there has been identified an association between CCT and intraocular pressure (IOP) readings using the Goldmann applanation tonomater, where thicker corneas correspond to higher IOP values and thinner corneas lower IOP readings (Kniestedt C, et al. 2005 and Tonnu PA, et al. 2005). In nanophthalmos patients this fact may lead to the misclassification of nanophthalmos associated glaucoma.

According to Karimian F *et al.* (2010), normal corneal keratometric values were defined as 44.11±1.47D. All Orbscan analyzed eyes (12 corneas) studied showed

maximum and minimum values higher than normal, above two standard deviations (2**σ=**48,52 D). There is no clear difference between probands (maximum diopter values ranged from 48,9 to 51,6 D, with an average of 49,7 D; and minimum values ranged from 48 to 50,1 D, with an average of 48,7 D). Increased corneal curvature may represent a corneal compensatory mechanism to minimize the final refractive error. Whether this is a result of direct genetic influence or a consequence of scleral structural changes (thicker than normal), remains to be clarified.

Despite the expansion of the mutational gene pool of *MFRP*, no clear genotype-phenotype correlation could be established in this large series of AR nanophthalmos. To the best of our knowledge, this is the largest series of nanophthalmos patients ever studied. A complete functional assessment of the different ocular structures will certainly improve our understanding of eye physiology and development.

References

1. Sundin OH, Dharmaraj S, Bhutto IA, Hasegawa T, McLeod DS, Merges CA, Silva ED, Maumenee IH, Lutty GA. Developmental basis of nanophthalmos: MFRP is required for both postnatal ocular growth and postnatal emmetropization. Ophthalmic Genet 2008; 19(1):1-9.
2. O'Grady RB. Nanophthalmos. Am J Ophthalmol 1971; 71:1251-1253.
3. Cross HE, Yoder F. Familial nanophthalmos. Am J Ophthalmol 1976; 81:300-306.
4. Othman MI, Sullivan SA, Skuta GL, Cockrell DA, Stringham HM, Downs CA, Fornes A, Mick A, Boehnke M, Vollrath D, Richards JE. Autosomal dominant nanophthalmos (NNO1) with high hyperopia and angle-closure glaucoma maps to chromosome 11. Am J Hum Genet 1998; 63:1411-1418.
5. Sundin OH, Leppert GS, Silva ED, Yang JM, Dharmaraj S, Maumenee IH, Santos LC, Parsa CF, Traboulsi EI, Broman KW, DiBernardo C, Sunness JS, Toy J,

Weinberg EM. Extreme hyperopia is the result of null mutations in MFRP, which encodes a frizzled-related protein. Proc Natl Acad Sci 2005; 102:9553-9558.

6. Li H, Wang JX, Wang CY, Yu P, Zhou Q, Chen YG, Zhao LH, Zhang YP. Localization of a novel gene for congenital nonsyndromic simple microphthalmia to chromosome 2q11-14. Hum Genet 2008; 122:589-593.
7. Panfeng Wang, Zhikuan Yang, Shiqiang Li, Xueshan Xiao, Xiangming Guo, Qingjiong Zhang. Mol Vis 2009; 15:181-186
8. Ayala-Ramirez R, Graue-Wiechers F, Robredo V, Amato-Almanza M, Horta-Diez H, Zenteno JC. A new autosomal recessive syndrome consisting of posterior microphthalmos, retinitis pigmentosa, foveoschisis, and optic disc drusen is caused by a MFRP gene mutation. Mol Vis 2006; 12:1483-1489.
9. Warburg M. Classification of microphthalmos and coloboma. J Med Genet 1993; 30:664-669.
10. Kimbrough RL, Trempe CS, Brockhurst RJ, Simmons RJ. Angle closure glaucoma in nanophthalmos. Am J Ophthalmol 1979; 88(3 Pt 2):572-579
11. Singh OS, Sofinski SJ. Nanophthalmos: guidelines for diagnosis and therapy. In: Albert DM, Jakobiec FA editors. Principles and Practice of Ophthalmology: Clinical Practice, Vol 3; Chapter 135. Philadelphia: WB Saunders, 1994:1528-1540.
12. Walsh MK, Goldberg MF. Abnormal foveal avascular zone in nanophthalmos. Am J Ophthalmol 2007; 143:1067-1068.
13. MacKay CJ, Shek MS, Carr RE, Yanuzzi LA, Gouras P. Retinal degeneration with nanophthalmos, cystic macular degeneration, and angle closure glaucoma: a new recessive syndrome. Arch Ophthalmol 1987; 105:366-371.
14. Hermann P. Le syndrome: microphtalmie-retinite pigmentaire-glaucome. Arch Ophtalmol Rev Gen Ophtalmol 1958; 18(1):17-24
15. Sener EC, Mocan MC, Sarac OI, Gedik S, Sanac AS. Management of strabismus in nanophthalmic patients: a long-term follow-up report. Ophthalmology 2003; 110:1230-1236.
16. Sugar HS, Thompson JP, Davis JD. The oculo-dento-digital dysplasia syndrome. Am J Ophthalmol 1966; 61(6):1448-1451.
17. Yardley J, Leroy BP, Hart-Holden N, Lafaut BA, Loeys B, Messiaen LM, Perveen R, Reddy MA, Bhattacharya SS, Traboulsi EI, Baralle D, De Laey JJ, Puech B, Kestelyn P, Moore AT, Manson FDC, Black GCM. Mutations of VMD2 splicing

regulators cause nanophthalmos and autosomal dominant vitreoretinochoroidopathy (ADVIRC). Invest Ophthalm Vis Sci 2004; 45:3683-3689.

18. Bergada I, Schiffrin A, Abu Srair H, Kaplan P, Dornan J, Goltzman D, Hendy GN. Kenny syndrome: description of additional abnormalities and molecular studies. Hum Genet 1988; 80:39-42.
19. Mukhopadhyay Rajarshy, Sergouniotis Panagiotis, Mackay Donna, Day Alexander, Wright Genevieve, Devery Sophie, et al. Mol Vis 2010; 16:540-548
20. Hashemi H, Yazdani K, Mehravaran S, KhabazKhoob M, Mohammad K, Parsafar H., et al. Cornea 2009; 28(4):395-400.
21. Karimian F, Feizi S, Doozandeh A, Faramarzi A, Yaseri M. J Refract Surgery 2010; 15:1-7
22. Dimasi D, Burdon K, Craig J. Br J Ophthalmol 2010; 94:971-6
23. Kniestedt C, Lin S, Choe J, et al. Arch Ophthalmol 2005; 123:1532-7
24. Tonnu PA, Ho T, Newson T, et al. Br J Ophthalmol 2005; 89:851-4
25. Metlapally Ravikanth, Li Yi-Ju, Tran-Viet Khanh-Nhat, Bulusu Anuradha, White Tristan, Ellis Jaclyn, et al. Mol Vis 2008; 14:387-393
26. Won J, Smith RS, Peachey NS, Wu J, Hicks WL, Naggert JK, Nishina PM. Vis Neurosci 2008; 25(4):563-574
27. Khan A, Zafar SN. J Pak Med Assoc. 2009; 59(11):791-3